

Supporting information

An atomistic view on carbocyanine photophysics in the realm of RNA

Fabio D. Steffen, Roland K. O. Sigel and Richard Börner¹

Department of Chemistry, University of Zurich, Winterthurerstrasse 190, 8057 Zurich, Switzerland

¹ author to whom correspondence should be addressed (richard.boerner@chem.uzh.ch)

Supplementary Methods

Activation energy from quantum yields

As a measure for the relative intensity of the fluorescence depopulation pathway, the quantum yield of sCy3 is defined as ⁷

$$\Phi_f = \frac{k_f}{k_f + k_{ic} + k_{N \rightarrow t}(T, \eta)} = k_f \tau \quad (3)$$

where k_f and k_{ic} are the rates of fluorescence and internal conversion respectively and $k_{N \rightarrow t}$ the rate limiting step of the photoisomerization reaction (for Cy3B $k_{N \rightarrow t} = 0$). Assuming both k_f and k_{ic} to be equal in sCy3 and Cy3B we can write

$$\Phi_f^{-1}(\text{sCy3}) - \Phi_f^{-1}(\text{Cy3B}) = \frac{k_{N \rightarrow t}(T, \eta)}{k_f}. \quad (4)$$

Modeling the temperature dependence of the isomerization reaction with the Arrhenius equation $k_{N \rightarrow t} = A \exp(-E_{N \rightarrow t}/RT)$ yields

$$\ln [\Phi_f^{-1}(\text{sCy3}) - \Phi_f^{-1}(\text{Cy3B})] = \ln (A/k_f) - E_{N \rightarrow t}/RT \quad (5)$$

Dynamic light scattering (DLS)

Experiments were carried out on a DynaPro Titan (Wyatt Technologies) equipped with a thermostat and a 50 mW laser operating at 827.8 nm. Data was collected at a scattering angle of 90° over a two second interval and averaged over 50 acquisitions. The autocorrelation function $g^2(\tau)$ is described in terms of the moments about the mean ⁸

$$g^{(2)} = B + \beta \exp \left(- 2\bar{\Gamma}\tau \right) \left(1 + \frac{\mu_2}{2!}\tau^2 + \frac{\mu_3}{3!}\tau^3 \right)^2 \quad (6)$$

where $\bar{\Gamma}$ is the mean decay rate, μ_2 and μ_3 the second and third moment about the mean, β the amplitude and B a y-axis offset. The decay rate Γ is given by $\Gamma = Dq^2$ with D being the diffusion coefficient and q the norm of the scattering vector

$$q = \frac{4\pi n}{\lambda} \sin \left(\frac{\theta}{2} \right). \quad (7)$$

Here, n represents the refractive index λ the laser wavelength and θ the scattering angle.

The diffusion coefficient again is related to the hydrodynamic radius r_h via the Stokes-Einstein equation

$$r_h = \frac{k_B T}{6\pi\eta D} \quad (8)$$

with the Boltzmann constant k_B , the absolute temperature T and the dynamic viscosity η .

From the overall tumbling the hydrodynamic radius r_h can then be computed as ⁹

$$r_h = \left(\frac{3k_B T \tau_r}{4\pi\eta} \right)^{1/3} \quad (5)$$

where η is the viscosity of the solvent, k_B the Boltzmann constant and T the absolute temperature. For the d3'EBS1* hairpin we derive a hydrodynamic radius of $21 \pm 1 \text{ \AA}$ which is in good agreement with the value from dynamic light scattering (DLS, $16 \pm 1 \text{ \AA}$, Supplementary Figure 4), given that the latter were performed without the dyes attached to the RNA.

Anisotropy decay from Monte Carlo (MC) sampling

Anisotropy decays were calculated on the basis of MD trajectories using a Monte Carlo algorithm.

1. sample the time of the excitation laser pulse t_0^k uniformly with $k=1,2,\dots,n$
2. sample the time point when the emitted photon hits the detector t^k , based on a probability distribution which is given by the lifetime decay $I(t) = \sum_i a_i \exp(-t/\tau_i)$ with $\sum_i a_i = 1$
3. calculate the angle $\theta(t-t_0)$ between the vectors of the absorption and emission transition dipole $\mu(t_0^k)$ and $\mu(t^k)$ respectively
4. determine the polarization of the incoming photon based on the probability $P(p) = |\cos(\theta)|$ for detecting a p -photon
5. increase the counter (+1) in either the s - or the p -polarization channel for arrival time $t_{\text{arrival}} = t^k - t_0^k$
6. bin the arrival times for the s - and p -channel independently
7. calculate the anisotropy $r(t)$ from the intensity $I_p(t)$ and $I_s(t)$ according equation 1, setting $G = 1$ and including an additional prefactor of 2/5 to account for photoselection in the ensemble experiment
8. correct for the viscosity of the water model by multiplying the arrival times with $c_{\text{diff}} = D_{\text{sim}}/D_{\text{exp}}$ where D is the self-diffusion of H_2O in the simulation (calculated from the mean square displacement) or the experimentally determined value¹⁰

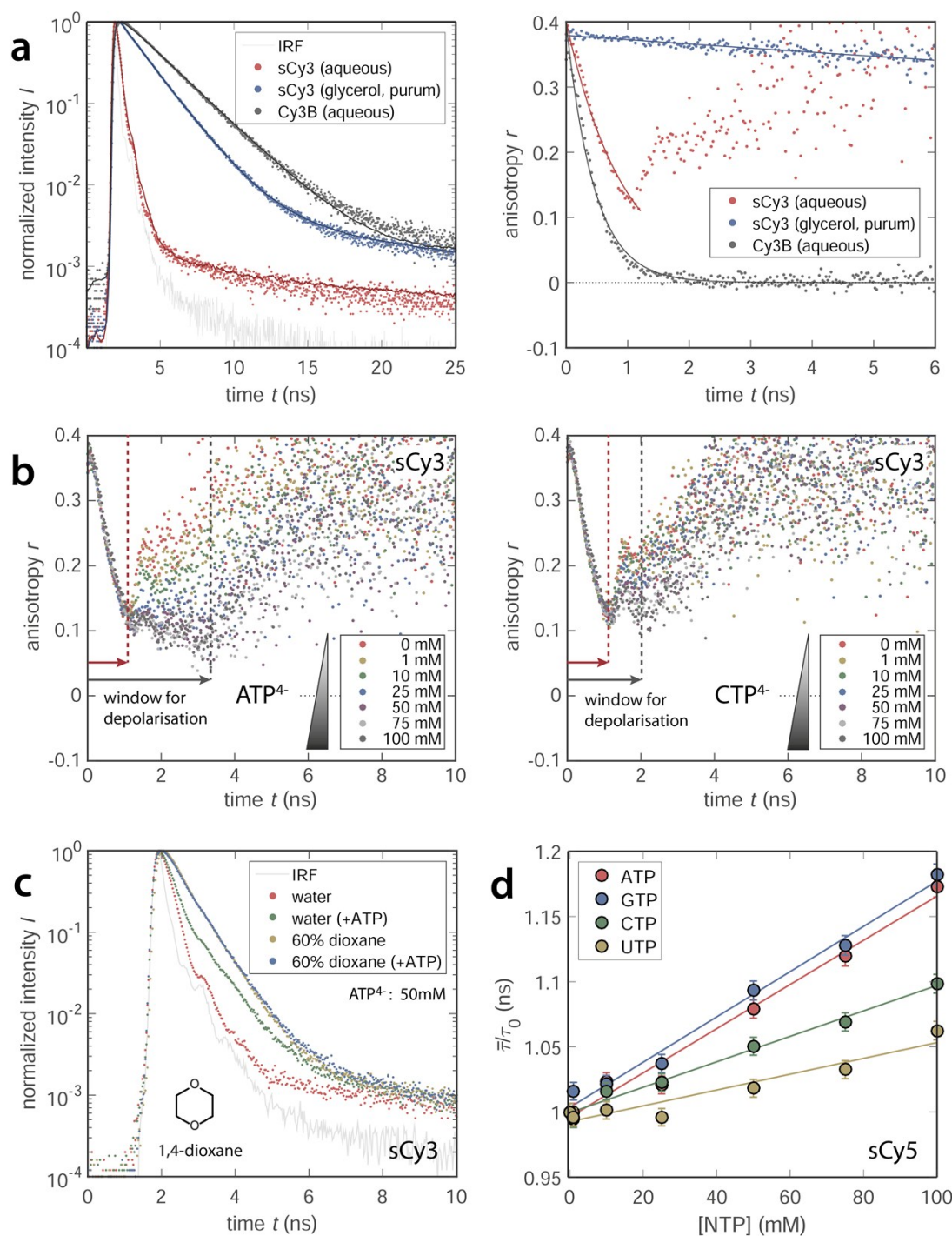
Table 1. Influence of K^+ on the fluorescence lifetime and dynamic anisotropy (divalent metal ions are chelated by 100 μ M EDTA).

	100 μ M EDTA			100 μ M EDTA + 100 μ M K^+		
	a_I	τ_I (ns)	τ_2 (ns)	a_I	τ_I (ns)	τ_2 (ns)
sCy3						
sCy3	–	0.17(1)	–	–	0.17(1)	–
sCy3-RNA-oligo	0.89(2)	0.29(2)	1.3(1)	0.88(3)	0.29(2)	1.3(1)
sCy3-DNA-oligo	0.92(3)	0.28(2)	1.4(1)	0.88(3)	0.26(2)	1.3(1)
sCy3-d3'EBS1*	0.79(3)	0.34(2)	1.7(1)	0.77(3)	0.36(2)	1.8(1)
sCy3-d3'dEBS1*	0.75(2)	0.38(2)	1.9(1)	0.72(2)	0.42(3)	2.0(1)
sCy5						
sCy5	0.35(2)	0.45(3)	0.88(4)	0.31(2)	0.32(2)	0.85
sCy5-RNA	0.48(2)	0.63(3)	1.6(1)	0.47(2)	0.62(3)	1.6(1)
sCy5-DNA	0.45(2)	0.58(3)	1.5(1)	0.44(2)	0.55(3)	1.6(1)
sCy5-IBS1*	0.54(3)	0.48(3)	1.5(1)	0.57(3)	0.49(3)	1.4(1)
sCy5-dIBS1*	0.42(2)	0.51(2)	1.4(1)	0.40(2)	0.50(3)	1.3(1)

Table 2. Photophysics of carbocyanine dyes in different microenvironments (50 mM K^+ , 10 mM Mg^{2+} , pH 7.5, 25°C, $r_0 \equiv 0.38$).

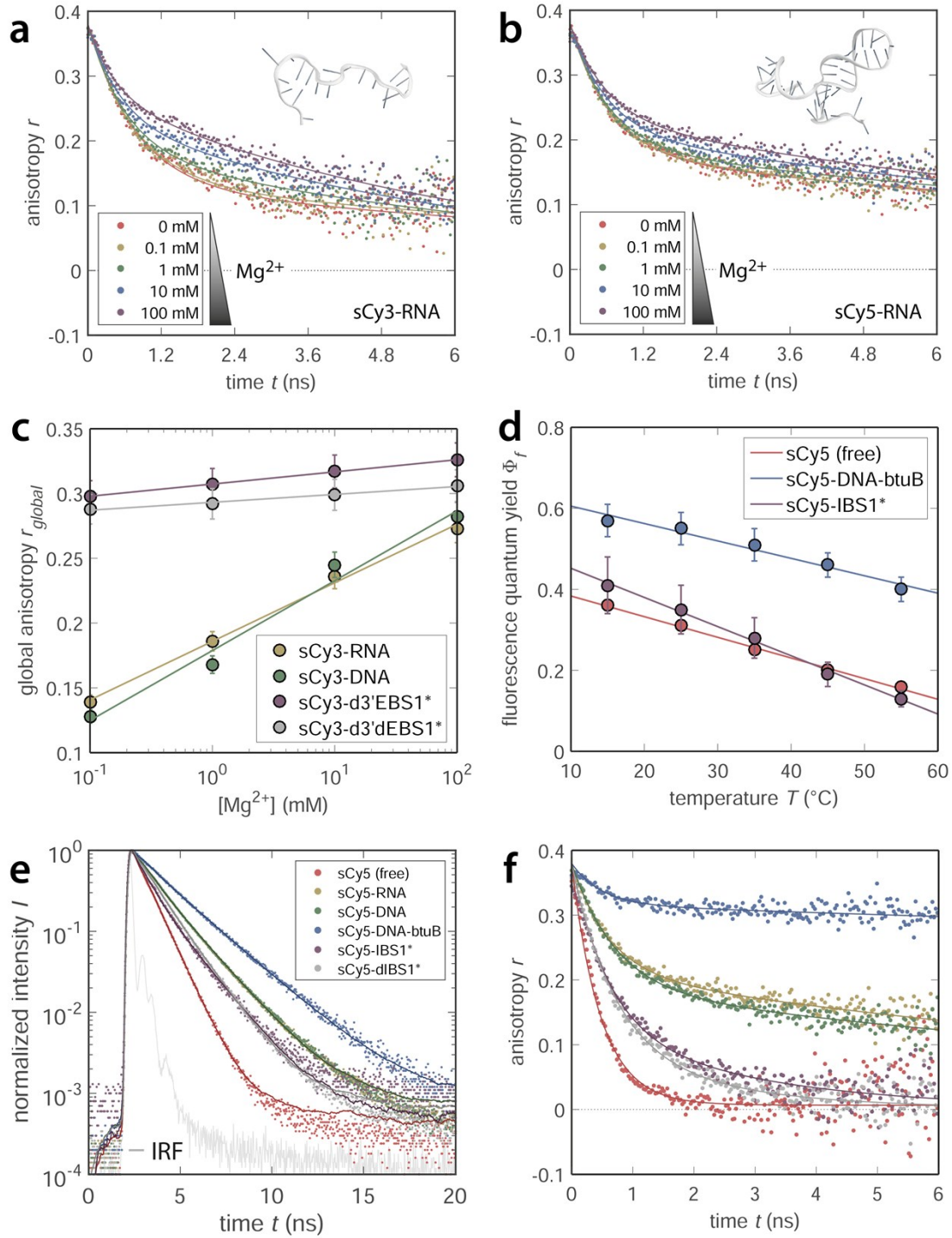
	a_I	τ_I (ns)	τ_2 (ns)	$\tau_{r,local}$ (ns)	$\tau_{r,global}$ (ns)	r_{global}	r_h (nm)	Φ_f
sCy3								
sCy3 (water)	–	0.17(1)	–	–	0.82(3) *	–	0.97(4) *	0.07(1)
sCy3 (glycerol)	0.37(2)	0.64(2)	1.9(1)	–	60(5)	–	0.40(3)	–
sCy3B	–	2.5(1)	–	–	0.46(2) **	–	0.80(3) **	–
sCy3-RNA-oligo	0.87(3)	0.30(2)	1.5(1)	0.55(2)	6.7(2)	0.24(1)	2.0(1)	–
sCy3-DNA-oligo	0.85(2)	0.32(2)	1.6(1)	0.55(2)	5.7(2)	0.25(1)	1.9(1)	0.20(1)
sCy3-DNA- <i>btuB</i>	0.73(3)	0.40(3)	1.7(1)	0.42(2)	30(3) **	0.29(1)	3.2(3) **	0.25(2)
sCy3-d3'EBS1*	0.72(3)	0.41(3)	1.9(1)	0.36(3)	8.9(4)	0.32(1)	2.1(1)	0.28(1)
sCy3-d3'dEBS1*	0.67(2)	0.44(3)	2.1(1)	0.55(2)	8.3(3)	0.30(1)	2.1(1)	–
sCy5								
sCy5	0.33(1)	0.36(2)	0.86(3)	–	0.50(2)	–	0.82(3)	0.30(1)
sCy5-RNA	0.45(2)	0.62(3)	1.7(1)	0.63(2)	13(2)	0.21(1)	2.4(4)	–
sCy5-DNA	0.46(2)	0.62(3)	1.7(1)	0.75(3)	14(2)	0.19(1)	2.5(4)	–
sCy5-DNA- <i>btuB</i>	0.31(1)	0.60(3)	2.2(1)	0.49(2)	>100 **	0.32(1)	> 4.8 **	0.53(4)
sCy5-IBS1*	0.65(3)	0.56(3)	1.5(1)	0.76(3)	2.9(2)	0.13(1)	1.5(1)	0.34(6)
sCy5-dIBS1*	0.40(2)	0.52(2)	1.3(1)	1.0(1)	2.4(3)	0.09(1)	1.4(2)	–

limited accuracy because of narrow observation time window (*) or very slow anisotropy decay (**).

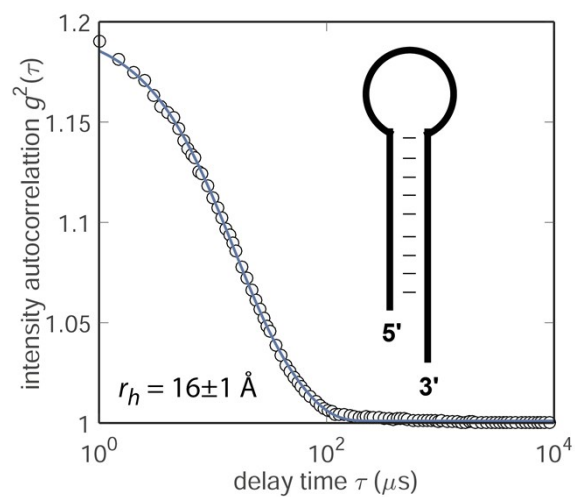


Supplementary Figure 1. Influence of the microenvironment on the photophysics of carbocyanine dyes. (a) Increase of the fluorescence lifetime (left) and dynamic anisotropy (right) of sCy3 upon restricting the torsion angle of the polymethine linker (viscosity of solvent or cyclization). (b) Broadening of the time window for fluorescence depolarization (as a result of a longer lifetime) upon addition of ATP⁴⁻ (left) or CTP⁴⁻ (right) with a background of 50 mM K⁺ and 3 mM Mg²⁺. (c) Effect of the solvent polarity on the interaction propensity of sCy3 and ATP. In a 60% 1,4-dioxane-water mixture addition of 50 mM ATP does not increase the fluorescence lifetime, hinting that stacking interactions between the dye and the nucleotide are reduced. (d) NTP titration displaying a relative increase of the fluorescence lifetime of sCy5 with respect to the initial value at 0 mM NTP (50 mM K⁺ and 3 mM Mg²⁺).

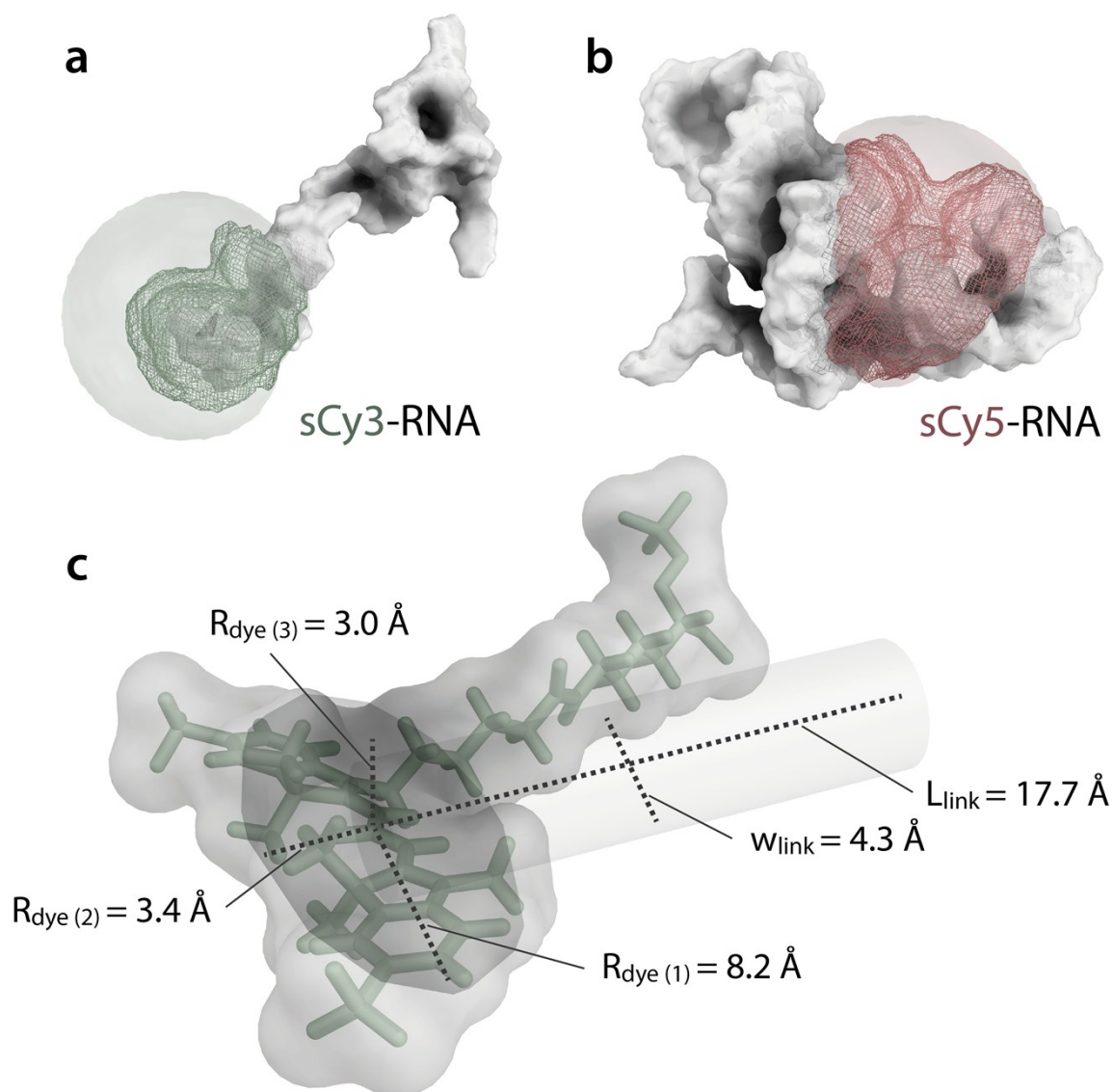
Supplementary Figure 2. Secondary and tertiary structures of the RNA constructs used in this study. (a) sCy3 modified d3'EBS1* with 3'-tetraU tail (melting temperature measured without the dangling end, $T_m = 49.4(2)^{\circ}\text{C}$ ¹; the NMR structure² (PDB 2m24) has been extended with a canonical tetraU overhang) (b) sCy5 labeled IBS1* (c) sCy3-RNA oligonucleotide complementary to the expression platform of the *btuB* riboswitch (secondary structure and T_m predicted by Mfold³, $T_m = 36^{\circ}\text{C}$; tertiary structure prediction by RNAComposer⁴) (d) sCy5-RNA oligonucleotide complementary to the 5'-elocation segment of the *btuB*. (Mfold prediction of entire sequence: $T_m = 63^{\circ}\text{C}$, for 5'-terminal stem loop: $T_m = 50^{\circ}\text{C}$) (e) Anti-aptamer (gene-on) conformation of the engineered *btuB* riboswitch which hybridizes to an sCy3-DNA and an sCy5-DNA oligonucleotide with a terminal biotin (B).^{5,6}



Supplementary Figure 3. Effect of metal ions and temperature on the photophysics of cyanine labeled nucleic acids. (a/b) Mg^{2+} titration with sCy3-RNA or sCy5-RNA in presence of 50 mM K^+ . Initially, all divalent metal ions are chelated by 100 μ M EDTA (0 mM Mg^{2+} , independent sample). (c) Linear increase of the residual anisotropy r_{∞} as a function of the Mg^{2+} concentration, corresponding to a larger amplitude (relative weight) of the global correlation time τ_{global} of sCy3 (higher interaction propensity with the RNA). (d) Quantum yield of sCy5 as a function of the temperature for different microenvironments. (e/f) Fluorescence lifetime and anisotropy decays of sCy5 conjugated to various RNA and DNA constructs (instrument response function (IRF) in gray; fundamental anisotropy $r_0 \equiv 0.38$; 50 mM K^+ , 10 mM Mg^{2+} , 25°C).



Supplementary Figure 4. Intensity autocorrelation function $g^2(\tau)$ calculated from dynamic light scattering (DLS) measurements for the hairpin d3'EBS1*.



Supplementary Figure 5. Accessible volume (AV) calculations of Cy-labeled RNAs. The contact volume (CV) is represented as a mesh within the AV cloud for (a) sCy3-RNA and (b) sCy5-RNA. (c) Parameterization of the sCy3 dye and the C6 amino linker. The fluorophore is modeled by an ellipsoid and a cylinder using a total of five distances ($R_{\text{dye(1-3)}}$, w_{link} , L_{link}).¹¹ The extension of the polymethine chain in sCy5 by one C-C double bond affords $R_{\text{dye(1)}} = 10.1 \text{ \AA}$.

References

- 1 D. Kruschel and R. K. O. Sigel, *J. Inorg. Biochem.*, 2008, **102**, 2147–2154.
- 2 D. Kruschel, M. Skilandat and R. K. O. Sigel, *RNA*, 2014, **20**, 295–307.
- 3 M. Zuker, *Nucleic Acid Res.*, 2003, **31**, 3406–3415.
- 4 M. Popenda, M. Szachniuk, M. Antczak, K. J. Purzycka, P. Lukasiak, N. Bartol, J. Blazewicz and R. W. Adamiak, *Nucleic Acid Res.*, 2012, **40**, e112.
- 5 G. A. Perdrizet, I. Artsimovitch, R. Furman, T. R. Sosnick and T. Pan, *Proc. Natl. Acad. Sci. U. S. A.*, 2012, **109**, 3323–3328.
- 6 M. Zhao, F. D. Steffen, R. Börner, M. F. Schaffer, E. Freisinger and R. K. O. Sigel, 2016, **to be submitted**.
- 7 M. E. Sanborn, B. K. Connolly, K. Gurunathan and M. Levitus, *J. Phys. Chem. B*, 2007, **111**, 11064–11074.
- 8 B. J. Frisken, *Appl. Opt.*, 2001, **40**, 4087.
- 9 B. Valeur, *Molecular fluorescence. Principles and applications*, Wiley-VCH, Weinheim, New York, 2002.
- 10 M. Holz, S. R. Heil and A. Sacco, *Phys. Chem. Chem. Phys.*, 2000, **2**, 4740–4742.
- 11 S. Kalinin, T. Peulen, S. Sindbert, P. J. Rothwell, S. Berger, T. Restle, R. S. Goody, H. Gohlke and C. A. Seidel, *Nat. Methods*, 2012, **9**, 1218–1225.